Investigating histone H3 Lys^4 and Lys^9 methylation in conditionally immortalized olfactory placode by Matrix-assisted Laser Desorption/ Ionization Time-of-flight Mass Spectrometry

Chung-Pu Wu

DEPARTMENT OF MOLECULAR AND CELL BIOLOGY
UNIVERSITY OF CAPE TOWN

Thesis submitted in partial fulfilment of the requirements for the degree of Master of Science

February 2002

Investigating histone H3 Lys^4 and Lys^9 methylation in conditionally immortalized olfactory placode by Matrix-assisted Laser Desorption/ Ionization Time-of-flight Mass Spectrometry

Chung-Pu Wu, Wolf Brandt, Nicola Illing and Hugh Patterton

ABSTRACT

Published studies have shown that distinctive site-specific histone H3 methylation patterns at lysine 9 and lysine 4 determine the formation of heterochromatin or euchromatin, respectively. The biological significance of lysine 4 and lysine 9 methylation of histone N-terminal tails was investigated in this study with a new approach. In this study, an assay was developed to measure the methylation levels of Lys^4 and Lys^9 of histone H3 purified from a conditionally-immortalized clonal cell line OP27, which was derived from the mouse olfactory placode. Having established the method, the shift in the methylation patterns of histone H3 Lys^4 and Lys^9 was then measured when the OP27 cell line was induced to differentiate into non-inducing olfactory neurons. This was achieved by using MALDI-TOF mass spectrometry in conjunction with site-specific endoproteinase digestion.

INTRODUCTION

In eukaryotic cells, genes are packaged in a complex structure called chromatin. The fundamental units of chromatin are the nucleosomes, which consists of 168 base pairs of DNA wrapped around the core histones (1). The core histones consist of lysine-rich H2A and H2B as well as arginine-rich H3 and H4. These histones are synthesized in the cytoplasm, transported into the nucleus, and assembled into nucleosomes. The primary amino acid sequence of each histone is highly conserved between the species, especially in H3 and H4 (1, 2). In general, there are two major domains in histones; the globular domain and the tail domain. Several post-translational modifications, including acetylation, ADP-ribosylation, methylation, ubiquitination and phosphorylation are known to take place at the tail domains of the histones (2-5). These histone tails are less structured, protease sensitive and protrude from the exterior of the chromatin structure. They are not essential for the nucleosome formation, but prove to be indispensable for nucleosome-nucleosome interaction (2, 5). Histones were once only thought of as static, non-participating structural elements, but it has now been shown not to be the case. The literature has suggested that histone modifications might alter chromatin structure and function, thus allowing dynamic changes in the accessibility of the underlying DNA by altering the protein-protein (histone-histone) and/or protein-DNA (histone-DNA) interactions at specific sites (5-7). These post-translational modifications are highly conserved throughout evolution and can act either synergistically or antagonistically. A classic example is the case where methylation at a lysine residue would prevent

acetylation at the same site and thus preventing gene activation and inhibiting the transcriptional process (8). Numerous studies have provided evidence that these covalent marks with distinct patterns may contribute to a more diverse and complex histone "language" (9-14).

Recent studies related to the post-translational modifications of histones yielded important insights into the dynamic nature of the chromatin structure and its fundamental role in gene expression. Unfortunately, other than acetylation, the roles of these modifications are still not well understood. Murray first described the ε-N-methylated lysine in histones as early as 1964 (15), but its precise functional significance still remains as one of the least understood post-translational modifications affecting histones. It is thought very unlikely that histone methylation is a random event without any functional or structural significance due to the fact that evolutionarily it has been highly conserved. Two approaches have been used to investigate the functional role of histone methylation. *In vitro* studies suggested that the transcriptional activity of DNA is inhibited by site-specific histone methylation, while further modifications such as acetylation and phosphorylation may reduce the effectiveness of the blockage. The other approach used *in vivo* studies to determine the temporal relationship between histone protein methylation, the synthesis of DNA, RNA and protein synthesis (16, 17).

Histone methylation is a covalent modification that occurs at arginine and lysine residues only. It is catalysed by histone methyltransferases (HMTs)

with S-adenosylmethionine (SAM) acting as a co-factor. SAM functions by donating the methyl group to the histone ε-N termini (18, 19). Protein-lysine methyltransferase (a Type III methylase) is one of the three major classes of enzymes that are responsible for the histone methylation. It methylates the lysine residues in histones. This methyltransferase can only be found in the nucleus, where it is tightly bound to the chromatin (20). Early work has shown that H3 and H4 are the primary histones modified by methylation and several lysines (residues 4, 9, 27 and 36 for H3 and 20 for H4) are the preferred sites (3, 21) that have been highly conserved. Each modified lysine can be mono-, di-, or tri-methylated (3). This stepwise methylation at the ε-amino group of lysine residues seems to be a progressive reaction performed by the same enzyme (20, 22). The lack of specificity of this enzyme was later observed when the isolated enzyme not only methylated the arginine residues, but methylated the lysine residues as well (23). This loss of specificity implies that the enzyme must be in a specific conformation or environment when performing H3 and H4 histone lysine methylation.

Various studies suggest that unlike acetylation, the methyl modification is an irreversible process (19). It is unlikely that a global histone demethylase (HDM) exists since there is no evidence suggesting a large decrease in methylated histones from bulk chromatin. However, it is still possible that demethylation of histones occurs on specific residues, but these activities still need to be discovered (14, 24). Specific lysine residues in H3 and H4 tails are normally targeted for either acetylation or methylation. However, lysine 9 residue (Lys9) in H3 tails has been shown to be targeted for both

modifications. It is possible that certain combinations of acetylation and methylation in histone tails may have either antagonistic or co-operative effects. An excellent example is that hyper-acetylated H4 from transcriptionally active chromatin is a preferential target of histone H3 methylation. This suggests a synergistically acting effect to promote transcription (25).

Several reports have suggested the fact that increasing methylation on histone tails (lysine and arginine residues) will increase their affinity toward DNA. Studies have shown that the addition of methyl groups on the ε-amino group of lysine (mono, di or tri) will lead to a progressive reduction in charge density; not by altering the charge of the amino group, but rather by enhancing the basicity and hydrophobicity of the lysine residue and thus reducing its ability to form hydrogen bonds (8). This demonstrates the possibility of the basic histone tails to be able to condense chromatin into a more compact and inactive structure. Therefore, methylation of histones may alter the interaction of the histone tails with DNA and/or chromatin-associated proteins thus affecting the nucleosomal structure and function (24).

It has also been postulated that histone methylation may contribute to the nucleosome assembly and condensation of the chromatin during mitosis. It was shown that histone methylation has little turnover and this modification is a widespread event in chromatin. An elevation of methylase activity also correlates with mitosis in synchronous cell cultures (26). There seems to be a correlation between the cell cycle and the methylation pattern. Studies of the

histone methylation in the regenerating rat liver cells has suggested that the maximum methylation occurs only after the majority of DNA synthesis has been completed (27). Other studies of Chinese Hamster ovarian cells show that methylation occurs largely during the G2 phase of the cell cycle. In the case of HeLa S-3 cells, almost no methylation occurred until the end of the S-phase (28). Approximately 3 hours after DNA-synthesis, histone methylation reaches its highest point with a positive correlation with the elevation of methylase III activity. Links can thus be drawn between the histone methylation and chromatin condensation or mitosis, primarily because the condensation process which starts in G2 phase through to metaphase in mitosis coincides with this increase in methylation (26). Other studies have suggested that histone methylation may play a more dynamic role and therefore could be involved in the regulation of transcription rather than in chromatin structuring (28). Studies have also shown a correlation between the increasing level of histone methylation and transcriptional activity of chromatin. So methylation may therefore help chromatin to stay in an unfolded state and maintain transcriptional activity (29).

Generally, the lysines of the N-terminal region of H3 will either be methylated or acetylated (30). The three major sites of acetylation are lysine 14, 18, and 23 while the major sites of methylation are lysine 4, 9, 27 and 36, where lysine 9 may be either acetylated or methylated (31). When it was found that the acetylated species of H3 and H4 complexed with active genes are selectively methylated, it was hypothesized that lysine methylation may provide a way to modulate the potential for histone acetylation, or that

acetylation occurred before methylation, and thus increased the methylase accessibility to chromatin. The accessibility and reactivity of lysine residues in the enzymatic methylation and acetylation reaction by the corresponding enzymes may be dramatically influenced by the prior modification of a lysine residue or a lysines in close proximity (30).

The transcriptional activity of *Tetrahymena* micronuclei does not correlate with HMT (histone methyltransferase) activity nor is there a link between HMT DNA replication and mitosis (21). Further studies have shown that histone methylation is also not coupled to mitosis in the system of micronuclei. At the same stage, isolated macronuclei display a potent H3-specific HMT activity. Therefore, histone methylation of H3 Lys4 appears to be localized specifically to macronuclei in all stages of the life cycle and thus suggests a link to the transcription process (21). Interestingly, acetylated isoforms of H3 and H4 are the preferential targets of histone methylation, suggesting that HMTs and HATs act synergistically to promote transcription by some unknown mechanism (25, 29). Another study suggests that H3 Lys9 methylation may play a role in both transcriptional activation and transcriptional silencing. This was implied when studies showed that a histone acetyltranferase CBP/p300 co-immunoprecipitates with a HMT (SET domain-containing CBP-associated ASH1 protein). The preferential methylation site of this HMT was found to be H3 Lys9 (32).

It is particularly crucial to understand the interplay between different histone tail modifications. Growing evidence suggest different modifications can

affect each other. Recent studies have shown that in *Tetrahymena*, phosphorylation of H3 Ser^{10} is essential for proper chromosome condensation and segregation (33). This phosphorylation was shown to correlate with transcriptional activation and facilitates acetylation of H3 Lys^{14} (34-36). In addition, H3 Ser^{10} phosphorylation was shown to regulate H3 Lys^{9} methylation, since methylation of H3 Lys^{9} by SUV39H1 was significantly inhibited when H3 Ser^{10} was used as a substrate (37) and H3 Lys^{9} methylation also inhibited subsequent H3 Ser^{10} phosphorylation.

In summary, H3 Lys^{9} methylation correlates well with gene silencing, inhibiting Lys^{9} acetylation and Ser^{10} phosphorylation, while H3 Lys^{9} acetylation and H3 Lys^{4} methylation correlates with transcriptional activation. Ser^{10} phosphorylation inhibits Lys^{9} methylation and facilitates Lys^{14} methylation, which in term inhibits Lys^{9} methylation and induces gene activation (34-36).

In this study, a neural cell line immortalized with the temperature sensitive allele of the SV40 Tag large T antigen (SV40 Tag) was used to study changes in methylation associated with neuronal differentiation. These modified neural cells rapidly divide at a permissive temperature of 33°C but cease to divide and start to differentiate in RA differential medium at non-permissive temperature of 39°C (38).

Although primary cultures have been used to study neuronal differentiation, they have drawbacks such as limited lifespan and being non-renewable. Immortalisation of the

cells with oncogenes was thus performed (38), which concomitantly results in a stable phenotype that could be induced to differentiate along a particular pathway.

Temperature sensitive simian virus 40 (SV40) is an immortalising gene that was introduced into the olfactory cell line that functions as a temperature sensitive switch for cell division. This systems is well suited to study the cell morphology changes in actively growing and the non-growing state (39). Such transformed cells actively grow at 33 °C, which can then be inactivated by a shift to the non-permissive temperature of 39 °C where they cease to grow. Such a system may be related to the process of neuronal differentiation allowing one to study the mechanisms involved in cell differentiation. The influence of retinoic (38) acid on the morphological changes of the cells and e change in histone methylation when cells were shifted from the permissive temperature of 33°C to the non-permissive temperature of 39°C (38) where also studied.

In order to study histone methylation in a mammalian cell line, a sensitive and highly discriminating method is required to detect the presence of mono-, di- and tri- methylated lysine residues in histone H3, thus allowing correlations to be made with cell differentiation. Protein analysis by matrix-assisted laser desorption ionization (MALDI), coupled to a mass analyser such as the time-of-flight (TOF) (40, 41) has been used extensively by many laboratories. This technique also provides sequence and linkage information when used in conjunction with post-source decay (PSD) analysis (42, 43). Therefore, PSD-MALDI-TOF provides the most direct, specific and rapid way for studying and analysing of these methylation patterns (44). Specific and accurate

patterns of methylation can be determined when MALDI-TOF is coupled with Endoproteinase digestion experiments allowing for accurate mass determination (45, 46).

By using the selected OP27 cell line, we are able to study the morphological changes when the cells are shifted from a permissive temperature to a non-permissive temperature where cell differentiate. The studying of shift in methylation level by the use of endoproteinase digestion and MALDI-TOF mass spectrometry were developed and optimised. The changes in Lys^4 and Lys^9 methylation levels can then be identified, quantitated and correlated to the changes in cell morphologies at different cell stages.

MATERIALS AND METHODS

Tissue culture techniques

Olfactory placode (OP27) cells were cultured in 75 cm^2 culture flasks in Dulbecco's modified Eagle's medium (DMEM) supplemented with 10% heat-inactivated foetal calf serum (FCS). The cells were maintained at the permissive temperature of 33°C in a humidified atmosphere of 10% CO_2 – 95% air. Medium was renewed every 2-3 days. Antibiotics such as penicillin (10,000 U/ml) at 100 U/ml and streptomycin (10mg/ml) at 100 µg/ml were often used at the permissive temperature. At room temperature, phosphate buffered saline (PBS) was used to wash the culture monolayers and trypsin-

EDTA (0.25% trypsin and 0.04% EDTA in PBS) was used to lift the cells and harvest these cells.

Retinoic acid-induced cell differentiation experiment

To induce cell differentiation, the OP27 cell line was grown to approximately 65% confluence in DMEM/FCS at 33°C. In order to synchronise the OP27 cell line prior to differentiation, the cells were treated with 100ng/ml colcemid and monitored over a period of 27 hours. Colcemid modifies the morphology of cell (become spherical) at certain growth phases decreasing their adhesion and consequently allowing them to be lifted and washed off. This synchronization process ensured that all the cells differentiate at the same time when shifted to a non-permissive temperature. Colcemid containing medium was removed and replaced with all-trans-retinoic acid (RA media) when more than 50% of the cells were rounded up. The RA media consists of 50:50 DMEM/F12 with 2% FCS, 1% N2-supplement (Gibco), 100μM ascorbic acid and 10μM of retinoic acid (38), which were replaced every 48 hours. The cells were immediately transferred into a non-permissive temperature of 39°C and harvested following different incubation periods (1, 3, 5 and 10 days). A more gentle technique was used to harvest the cells when incubated at 39°C, due to the fact that they are much more fragile and may be degraded by trypsin-EDTA. Thus cell monolayers were first washed gently with PBS, scraped off with a cell scraper and collected with saline-EDTA.

Light microscopy

OP27 cells were checked each day with an Olympus CK40 inverted microscope fitted with 10x objective, contrast field filter and a JVC colour video camera. For the purpose of morphological studies, cells were grown in the 75 cm^2 culture flasks and

photographed directly in these flasks daily at 10x magnification. AnalySIS soft imaging system software was used to analyse the captured photographs.

Isolation of total histone from mouse brain tissues

Mice were killed by cervical blow and all procedures were carried out at 4°C. Brains were chopped up with scissors and homogenized with 0.32M sucrose-TKM (Tris, potassium and magnesium containing sucrose solution) (pH 7.5) in a Dounce homogeniser. The mixture was filtered through 2 layers of cheese-cloth and spun down. The pellet was resuspended in 1.7 M sucrose-TKM, spun down and removed the supernatant fluid carefully. Pellet was then resuspended in 2.3 M sucrose-TKM, spun down and the final pellet containing nuclei was collected. The pellet was washed with 0.15 M NaCl solution before re-dissolved in 1 ml of water. Concentrated HCl (10 M) was added and mixed to reach the final concentration of 0.4 M. Supernatant was collected after spinning and ready for HPLC purification.

Isolation of total histone from OP27 cell-line

3.52×10^6 of OP27 cells were cultured and collected in Dulbecco's modified Eagle's medium. The cell pellet was homogenised with saline-EDTA (pH 8.0) using Polytron homogeniser (supplied by KINETICA). After centrifugation, the pellet was washed successively with saline-EDTA and 0.05M Tris-buffer (pH 8.0). The pellet was then further homogenised with 0.05M Tris-buffer using the Dounce homogeniser. The final pellet was resuspended with Tris-buffer, layered over a 0.5M sucrose solution and centrifuged through the sucrose solution. The final pellet was washed with 0.5M

NaCl solution, spun down and re-suspend in 1ml of Milli-pore water. Histones were acid extracted by adding 40µl of 10M HCl stock solution to the 1ml solution to a final concentration of 0.4M. The supernatant was collected after centrifugation, and stored at 4°C.

Histone H3 isolation by reversed-phase high performance liquid chromatography (RP HPLC)

The supernatant containing total histones was separated onto a Jupiter 5µ C18, 300Å column connected to a Waters HPLC pump where the total histones were separated into individual histone fractions. Chromatography was performed using a two eluent buffer system. Buffer A consisted of an aqueous solution of 0.1% TFA, and buffer B consisted of an aqueous solution of 0.1% TFA with 70% acetonitrile. The reversed-phase HPLC analyses were performed using the following gradient conditions, flow rate of 0.7 ml/min, 0-100% B over a period of 65 minutes, held at 100% B for 5 minutes, and back to 0% B over 20 minutes. Histone H3 was purified by manual peak collection. Fractions of H3 were collected at 89% B over a period of 1 minute, corresponding to a fraction volume of 0.7 ml at a flow rate of 0.7 ml/min. The collected fractions were later confirmed by Matrix-Assisted Laser Desorption Time of Flight Mass Spectrometry (MALDI-TOF MS).

Endoproteinase Arg-C digestion

Endoproteinase Arg-C is a cysteine protease that cleaves peptide bonds specifically at the C-terminal end of arginine residues. The histone H3 protein was first dissolved in

an incubation buffer (100mM Tris-HCl, 10mM $CaCl_2$, pH 7.6) and was then mixed with 1µl of Endoproteinase Arg-C, 2µl of activation solution and diluted to 20µl with incubation buffer. The histone H3 protein was incubated at room temperature for 4 hours before placing directly onto the MALDI target.

MALDI-TOF mass spectra techniques

Sample preparation for MALDI-TOF. 1 µl of sample solution was mixed with 1µl of α-CHC (α-cyno-4-hydroxycinnamic acid) Matrix solution (10 mg/ml in 6:3:1 acetonitrile : water : 3% TFA) and placed directly on the MALDI target. The mixture was then air-dried. *Instrumentation.* All MALDI-TOF mass spectra were acquired in ion linear mode on the HP G2030A MALDI-TOF MS system equipped with time-lag focussing using 20 kV accelerating voltage. Data were acquired and processed using PerSeptive Biosystems software.

RESULTS AND DISCUSSION

Culturing of the olfactory epithelium OP27 at 33 °C

OP27 cells grow at 33°C as a homogeneous cell population with a population doubling time (PDT) of 52 hours at 33°C (38), defined as the time, in hours, taken for the cell number to double (47). The cell culture consists of large, flat, irregular shaped cells and multinucleated cells are frequently encountered as shown in Figure 1. The longer they are maintained in the culture at 33°C, the more prominent the multinucleated cells became.

Induced cell differentiation and morphological changes occurring at the non-permissive temperature of 39 °

The OP27 cell line was originally kept in DMEM with 10% FCS at 33°C. OP27 cells were first treated with colcemid for 27 hours prior to changing the medium to RA medium and shifting to 39°C. Colcemid was used to synchronise cells and to ensure that all the cell differentiation occurred at the same time. The first sign of OP27 cell differentiation was that the original flat looking cell body started to round up and adopted a bipolar appearance with extension at both ends as shown in Figure 1 (Day 2-Day 4). Approximately 50 % of the cell culture died off initially and only stabilised in RA medium after 24 hours. After shifting and culturing cells in RA media at 39°C for the first 4 days (Fig 1, Day 0-4), the surviving cells looked reasonably healthy with some noticeable morphological changes. The cell body seemed to be reduced in size and elongated to a spindle-shaped appearance with long extensions growing

toward the neighbouring cells. After 6 days in culture at 39°C, the cell body looked fragile and got even smaller with its long needle-shaped extensions reaching out from both sides, contacting the neighbouring cells and in alignment with one another (Fig 1, Day 6). After an additional 3 days, the morphology of the cells remained unchanged, but numerous cell debris appeared in the medium and the cells exhibited an unhealthy appearance in that they became progressively more spherical. (Fig 1, Day 9- Day 10). This is due to the culture is being maintained at 39°C for a lengthy period. The thermolabile SV40 Tag protein in OP27 is degraded, correlating with the rapid increase in cell differentiation (48). Finally cell proliferation ceased when and cell death finally ensued.

Isolation, purification of histone H3 from OP27 cell line by reverse phase HPLC and molecular weight determination

Total histones were isolated via a modified isolation method followed by HCl acid extraction as detailed in the Materials and Methods. This method allows one to extract histones from the tissue culture cells directly and efficiently in comparison to the traditional extraction method which is not suitable for very small sample amounts. A total of 9 extractions were performed with the modified method to ensure the reproducibility. Although this particular extraction method has proved to be reliable for tissue cultured cell lines, it was found to be unsuitable for fresh animal tissues. The purity of the extracted histones was first assessed by means of sodium dodecyl sulphate polyacrylamide gel electrophoresis (SDS-PAGE) in Figure 2.1. In which the mouse liver total histones and the olfactory placode total histones were compared. Histones were then separated and purified by HPLC on a reverse phase C18 column

as indicated in the materials and methods section. Figure 2.2 shows that most of the histone H3 was eluted at 61 minutes with a linear gradient. Other fractions were eluted at the 55th minute, 56th minute and 58th minute as detailed in Table 1. The accurate molecular weights were determined by MALDI-TOF mass spectrometry, which allowed the identification of all four core histones (Fig 2.2B). Approximately 0.7 ml of histone H3 fraction was collected each time, dried under vacuum and subjected to the Endoproteinase Arg-C digestion. MALDI-TOF was then performed and generated the characteristic +14 Da mass ladders in some of the peptide fragments, the degree of methylation could be estimated. In order to quantitate the relative amount of the methylated lysine residues, it was assumed that the induction of the methyl groups had no effect on the signal strength. Even if the assumption is not valid, relative amounts of these derivatives in various cell stages should still reveal variations in this modification.

Enzymatic digestion, mass spectrometry and quantification of H3 methylation at Lys^4 and Lys^9 residues

All the eluted fractions from HPLC were first examined by using MALDI-TOF to identify the respective contents of the various peaks as shown in Figure 2.2B. Histone H2B, H4, H2A and H3 has a MH^+ of 14040.7 Da and MH^+ of 13805.0 Da, 11304.4 Da and 15320.1 Da respectively. Histone H3 was isolated and then subjected to Endoproteinase Arg-C digestion at room temperature prior to MALDI-TOF analysis as detailed in the materials and methods section. Figure 3A shows patterns of +14 Da mass ladders, which reveal the degree of methylation at lysine 4 and lysine 9 residues. This mass spectrometry pattern was compared to the theoretical values generated by

softwares, such as GPMAW (General Protein/Mass Analysis for Windows), in order to analyse how accurate the peaks were in comparison to the theoretical peaks. To further confirm the identity of these methylated peaks, Post source decay (PSD) spectra was also performed on the methylated mass peaks and were then matched to NCBI nonredundant database entries (data not shown). The results obtained shown most of the actual mass fragments coincide with the theoretical mass fragments generated, which also means that sufficient material could be isolated from a 75 cm^2 flask of OP27 cells to determine the profile of methylation at Lys^4 and Lys^9 of histone H3. This showed that the combination of Endoproteinase Arg-C / MALDI-TOF analysis is accurate enough for the purpose of this study and further experiments were then carried out with the same methodology.

Table 2 summarizes the representation of various peak masses and their relative abundances. The relative heights of their centre mass values were used as a representation of their relative abundances. Figure 3A represent one of the typical MALDI-TOF mass spectra after endoproteinase Arg-C digestion. Peak with a mass-to-charge ratio of 932.35 m/z corresponding to a short fragment (amino acids 1-8) with calculated MH^+ of 932.07 Da was used as a representation for the abundance of H3 Lys^4 and its mono-methylated Lys^4 was represented by a mass peak of 946.20 Da with calculated MH+ of 946.07 Da. Two distinct methylation ladders seemed to overlap each other at the 1800 Da region (Fig 3A). The first methylation ladder started at 1815.87 Da, which corresponding to the fragment containing both Lys^4 and Lys^9 methylation sites (amino acids 1-17). The addition of 14 mass units ($+CH_3$ –H) may be contributed by either Lys^4 or Lys^9, or both. The methylation ratio of this fragment is proportional to the individual peaks containing Lys^4 or Lys^9 and thus the degree of

methylation of the Lys^4 and Lys^9 was determined based only on the two fragments which contained single methylation sites 4 and 9 respectively. Peak at 1870.04 m/z with the calculated MH^+ of 1870.21 Da corresponds to the overlapping second digestive fragment (amino acids 9-26) and it was used to quantitate the abundance of H3 Lys^9. The following peaks with an addition of 14 mass units such as MH^+ of 1885.20 Da, 1899.41 Da and 1913.62 Da correspond to peptide masses containing mono-, di- and tri-methylated Lys^9's residues (Fig 3A and 3B). These peaks were used to quantitate the extend of methylation of histones H3 and H4 due to the fact these fragments were very prominent during the MALDI-TOF analysis. Although other methylated fragment where also apparent, they were not used as they could not always be unambiguous be identified. Another "methylation ladder" was also found at the region of 2784 Da (Fig 3A and 3B), which represents a long fragment of 26 amino acids (amino acids 1-26). This particular fragment consists of lysine residues 4 and 9, which can be methylated, as well as lysine 14 and 23, which can be acetylated. Analysis on this fragment was not considered since the data obtained at this stage was not sufficient to solve all the possible combinations. We quantitate these mass peaks and the +14 ladders obtained by MALDI-TOF analysis by their relative mass peak heights. Three independent experiments from three separate preparations were obtained and averaged, which indicated that while culturing OP27 cells at the permissive temperature (33 °C), 42.56 % of the Lys^4 and 75.85 % of the Lys^9 were methylated. For Lys^4, only mono-methylation was detected where as for Lys^9, 24.48 % were mono-methylated, 29.50 % di-methylated and 21.55 % were tri-methylated.

Methylation pattern analysis of partially differentiated and fully differentiated OP27 cells

At the beginning of the differential experiment, OP27 cells were treated with RA media and shifted to a non-permissive temperature where the SV40 Tag is inactivated and proliferation ceases. The HPLC elution profile in Figure 4.1A and the photos in Figure 1 both indicate that many of the OP27 cells died off and their histones started to degrade by proteases during a lengthy period at a non-permissive temperature. Although the same reverse phased column and HPLC system was used for Days 0-5, the elution profiles were vastly different. For Day 0 and Day 1, the profile looked largely the same, but for Day 3 and Day 5, histones seemed to be degraded and the collection of the histone H3 fraction became extremely difficult. There are two possible reasons for this; it is possible that the histone tails got degraded by proteases during the long incubation time and thus the typical N-terminal fragments were not found in MALDI-TOF analysis for Day 3 and Day 5. The second possibility is that OP27 cells die off, if exposed to RA media for a lengthy period of time. Thus the amount of cells harvested after Day 3 is simply insufficient to perform the MALDI-TOF analysis and the identification of N-terminal fragments becomes impossible. To investigate this matter further, study with 3 day differential period was done with addition of various proteases inhibitors. Due to the time constrain these experiments could not be completed.

The MALDI-TOF analysis in Figure 4B showed the normal methylation profile for Day 0, Day 1, Day 3 and Day 5, where Day 0 represent 27 hours after treating cells with colcemid, Day 1, Day 3 and Day 5 correspond to 24 hours, 72 hours and 120 hours after colcemid treatment respectively. Similar enzyme digestive patterns were obtained, but there were no signs of any N-terminal methylation for Day 3 and Day 5

(Fig 4B). This was further investigated with SDS-PAGE as shown in Figure 4.2A, where much lower histone H3 contents were observed in both Day 3 and Day 5. It was first thought that the quantities in the collected histone H3 HPLC fractions for day 3 and day 5 were too little and thus insufficient for MALDI-TOF analysis. After scaling up the experiment with significantly higher concentrations in each fraction, the more reasonable explanation seems to be that the protruding, more hydrophilic N-terminal histone tails were trimmed off by enzymatic proteolytic degradation and was probably degraded completely after day 3 by proteases released from cell debris. Thus no methylation pattern at the termini can be detected and only the core hydrophobic region of the histone H3 was analysed.

It is interesting that the relative amount of the histone H3 variant H3.2 (Fig 4.1A), determined by the height of the peak in the HPLC profile, went up from 35.63 % to 38.13 % during the course of 24 hours in RA medium. This variant is a replication dependent variant that is usually induced at the beginning and repressed at the end of DNA synthesis (49). The MALDI-TOF analysis results presented in Table 2 show an overall increase in methylation level at both H3 Lys^9 and Lys^4 residues after 24 hours at 39 °C in comparisons to the actively dividing cells. This result correlates nicely with the literature findings (3, 21, 50). Figure 4.2B shows the relative abundances of the methylation at Lys^4 (K4) and Lys^9 (K9) before treating with cell-differentiation medium and 24 hours after cell-differentiation medium treatment. The relative abundance of the non-methylated and mono-methylated K9 for Day 1 seems to be less than Day 0 with more di-methylated and tri-methylated Lys^9. A possible explanation is that some K9 got methylated into mono-methylated K9 during the first 24 hours, but at the same time, more mono-methylated K9 also got methylated into di-

methylated and later the same way to tri-methylated K9 by the same histone methyltransferases (HMT) (3, 21, 50). This result reinforced the theory that an increase in lysine 9 methylation is correlated with cell differentiation and transcriptional inactivation (21, 50). In this study the percentage of methylated Lys^4 is also increases and parallels the behaviour of Lys 9. This contradicts observation in the literature (21, 50) which postulates that an increase in Lys 4 methylation correlates with an activation in transcriptional acivity. Since there is still no evidence suggesting the existence of global histone demethylase (HDM) (21) Lys methylation appears to be a permanent and irreversible process that may explain the permanent nature of the differentiated state of cells like neurons. The results and conclusions obtained in these initial and limited studies are not yet that reliable, nevertheless it would appear that MALDI-TOF analysis may be an effective tool to study histone modifications and the transcriptional activity of cells.

Isolation, purification of histone H3 from mouse brain tissues

To ensure that this MALDI-TOF methodology works with both tissue cultured cell lines and fresh tissue samples, fresh mouse brains were used to confirm the quatitative determination of methylated lysine residues in histone. Previous studies have used amino acid analysis to show that the total histones and lysine residues in histone H3 of an animal's brain are highly methylated (51), thus mouse brain tissue was chosen for reference purposes. Three brain samples were extracted by the traditional method as described in Materials and Methods, then purified and analysed by MALDI-TOF MS exactly the same way as in OP27 cells. Methylation patterns for Lys^4 and Lys^9 of mouse brain cells were obtained as shown in Figure 5A. The difference in mouse

brain cells is that the Lys^4 residues are heavily methylated in comparison to OP27 cells. The Lys^4 residues are not only mono-methylated, there are high levels of di- and tri-methylated Lys^4 as well. Figure 5B compares an overall and individual methylation levels in mouse brain cells and OP27 cells. The percentage of overall methylated Lys^4 for mouse brain cells are approximately 35% higher than the OP27 cells, but interestingly, the overall methylated Lys^9 levels are exactly the same for both cell types (fig5B). Figure 5B shows that all the methylated Lys^4 residues are mono-methylated for OP27 cells, where mono-, di- and tri-methylated Lys^4 occur in mouse brain cells. Even though the overall Lys^9 methylation level was the same for both cell types, the mouse brain cells seemed to be more methylated than OP27 cells due to the higher percentage of tri-methylated Lys^9. It has been shown that methylase activity is much higher in liver and brain extracts from young animals than from old animals (52) and is consistent with observations of increasing methylation in differentiated OP27 cells. Table 3 summarised the relative abundance of various methylated and un-methylated lysine residues. It is evident that the overall methylation level of histone H3 increased for the differentiated OP27 cell line (Day 1) at both Lys^4 and Lys^9. It has also been show that the percentage of histone H3 lysine methylation is the lowest in the rapidly dividing mouse erythroleukemia (MEL) cells, higher in the spleen and increases to approximately double that of the MEL cells in the liver and brain tissues, which are fully differentiated (51).

CONCLUSIONS

A novel approach to study histone methylation patterns was tested in this study. It is achieved by site-specific enzymatic cleavage in conjunction with the highly accurate MALDI-TOF MS analysis of the fragmentation spectrum, which isolates the peptides containing lysine residues 4 and 9 with distinct methylation patterns. The unique +14 Da mass ladders may easily be identified as the distinct Lys^4 or Lys^9 methylation patterns as well as the degree of methylation (mono-, di and tri-) in OP27 cells can also be measured. This method is incredibly reliable in the sense that the results obtained were very reproducible in both olfactory placode cell line and mouse brain tissues. In this study, it has also been shown that cell differentiation can be induced chemically and may be used as a tool in the future studies. Links between the methylation levels to the corresponding morphological changes at various stages of cell differentiation may also be determined with the similar strategy used in this study. The mouse brain methylation study further confirms the reproducibility and reliability of the MALDI methodology, where terminally differentiated cells such as mouse brain cells, were found to be more methylated at both Lys^4 and Lys^9 in line with results obtained by amino acid analysis (51). Discrepancies in the quantitation of methylated lysine residues may be due the fact that not all the modified lysine residues in histone H3 had been studied.

ACKNOWLEDGMENTS

I thank F. Davids for assistance in tissue culture and A. Fiedler for assistance in mass spectrometry. I am grateful to N. Illing, H. Patterton and W. Brandt for their assistances, critical reading and suggestions on the manuscript.

REFERENCES

1. Kornberg R.D. and Lorch Y. (1999) *Curr Opin Genet Dev*, **9**:148-151.
2. Luger, K, and Richmond, T. J. (1998) *Curr. Opin. Genet. Dev.* **8**, 140-146.
3. van Holde, K. E. (1989) *Chromatin*, Springer-Verlag, New York
4. Wolffe, A. P. (1997) *Nature*, **387**, 16-17.
5. Wolffe, A. P. and Hayes J.J (1999) *Nucleic Acids Res*, **27**: 711-720.
6. Hansen, J. C., Tse, C. and Wolffe, A. P. (1998) *Biochemistry* **37**, 17637-17641.
7. Allan, J., Harborne, N., Rau, D.C and Gould, H. (1982) *J. Cell Biol.* **93**, 285-297.
8. Byvoet, P., and Baxter, C.S. (1975) *Academic Press, Inc,* New York, pp 127-151. (Stein, G.S., and Kleinsmith, L.J. Eds)
9. Turner, B.M. (1993) *Cell*, **75**, 5-8.
10. Mizzen, C. (1998) *Cold spring Harb. Symp. Quant. Biol.* **63**, 469-481.
11. Tordera, V. Sendra, R. and Perez-Ortin, J. E. (1993) *Experientia* **49**, 780-788.
12. Loidl, P. (1994) *Chromosoma* **103**, 441-449.
13. Lopez-Rodas, G. (1993) *FEBS Lett.* **317**, 175-180.
14. Jenuweint, T. and Allis, C. D. (2001) *Science*: **10**: 293 (5532): 1074-80.
15. Murray, K. (1964) *Biochemistry* **3**: 10-15.
16. Elgin, S. Froehner, R. Smart, J. and Bonner, J., (1971) *Adv. Cell. Mol. Biol.*, **(1).** 1
17. Allfrey, V., Faulkner and Mirsky, A., (1964) *Proc. Natl. Acad. Sci.*, U.S.A., **51**, 786.
18. Byvoet, P. (1972) *Arch Biochem Biophys*, **152**: 887-888.
19. Byvoet P., Shepherd G.R., Hardin J.M. and Noland B.J. (1972) *Arch Biochem Biophys*, **148**: 558-567.
20. Wallwork, J. C., Quick, D. P. and Duerre, J. A. (1977) *J. Biol. Chem.* **252**, 5977-5980.

21. Strahl, B. D., Briggs, S. D., Cook, R. G., and Allis, C. D. (1999) *Proc. Natl. Acad. Sci.* **96**: 14967-14972.

22. Waterborg, J. H. (1993) *J. Biol. Chem.* **268** (7), 4918-492.

23. Aniello, F., Branno, M., Giuseppe, G. and Tosi, L. (1989) *Biochemica et Biophysica Acta* **1008**, 31-38.

24. Rice J.C. and Allis C.D., (2001) *Curr Opin Cell Biol.* Jun; **13(3)**: 263-73.

25. Annunziato A.T., Eason M.B. and Perry C.A. (1995) *Biochemistry*, **34**: 2916-2924.

26. Honda, B. M., Candida, P. M., and Dixon, G. H., (1975) *J. Biol. Chem.* **250**, 8686-8689.

27. Tidwell, T., Allfrey, V. G., and Mirsky, A. E. (1968) *J. Biol Chem.* **243**, 707-715.

28. Borun, T. W., Pearson, D., and Paik, W. K. (1972) *J. Biol. Chem.* **247**, 4288-4298.

29. Hendzel M.J. and Davie J.R. (1989) *J Biol Chem*, **264**: 19208-19214.

30. Waterborg, J. H. (1990) *J. Biol. Chem.* **265 (28)**, 17157-17161.

31. Brandt, W. F., and von Holt, C. (1974) *Eur. J. Biol. Chem*, **46**, 419-429.

32. Bantignies F., Goodman R.H. and Smolik S.M. (2000) *Mol Cell Biol*, **20**: 9317-9330.

33. Wei, Y., Yu, L., Bowen, J., Gorovsky, M.A., and Allis, C.D. (1999) *Cell*, **97**: 99-109.

34. Sassone-Corsi, P., Mizzen, C.A., Cheung, P., Crosio, C., Monaco, L., Jacquot, S., Hanauer, A., and Allis, C.D. (1999) *Science* **285**: 886-891.

35. Cheung, P., Tanner, K.G., Cheung, W. L., Sassone-Corsi, P., Denu, J.M. and Allis, C.D. (2000) *Mol. Cell* **5**: 905-915.

36. Lo, W.S., Trievel, R.C., Rojas, J.R., Duggan, L., Hsu, J.Y., Allis, C.D, Marmorstein, R., and Berger, S.L. (2000) *Mol. Cell* **5**: 917-926.

37. Rea, S., Eisenhaber, F., O'Carroll, D., Strahl, B.D., Sun, Z.W., Schmid, M., Opravil, S., Mechtler, K., Ponting, C.P., Allis, C.D., et al. (2000) *Nature* **406**; 593-599.

38. Illing, N. Boolay, S. Siwoski, J. S. Casper, D. Lucero, M. T. and Roskams, J (2002) *In Press*.

39. Cacciotti, P and Libener, R (2001) *PNAS*: **9, 98(21)**: 12032-12037.

40. Mock, K. K., M. Davey and Cottrell J. S. (1991) *Biochem. Biophys. Res. Commun.* **177**, 644.

41. Stahl, B., Steup, M., Karas M. and Hillenkamp, F. (1991) *Anal. Chem.* **63**, 1463.

42. Spengler, B., Kirsch, D., Kaufmann R. and Lemoine, J. (1995) *J. Mass Spectrom.* **30**, 782.

43. Lemoine, J., Chirat, F. and Domon, B. (1996) *J. Mass Spectrum.* **31**, 908

44. Gobom J, Nordhoff E, Mirgorodskaya E, Ekman R, Roepstorff P, (1999) *J. Mass. Spectrum*: **34(2),** 105-116.

45. Andreozzi L, Federico C, Motta S, Saccone S, Sazanova AL, Sazanov AA, Smirnov AF, Galkina SA, Lukina NA, Rodionov AV, Carels N, and Bernardi G. (2001) *Chromosome Res*. **9(7):** 521-32.

46. Pieles U, Zurcher W, Schar M, Moser HE. (1993) *Nucleic Acids Res*. Jul **11;21(14)**:3191-6..

47. David, J.M. (1994) *Basic cell culture. A practical approach*. New York, IRL press, Oxford University Press.

48. Tegtmeyer, P. (1975) *J. Virol.* **15**: 613-618.

49. Zweidler, A. (1984) *Histone Genes* pp. 339-371, J. Wiley & Sons, N. Y. (Stein, G. S., Stein, J.L. & Marzluff, W. F., eds.)

50. Gary, J. D. and Clarke, S. (1998) *Prog. Nucleic Acid Res. Mol. Biol.* **61**: 65-131.

51. Lloyd, B. L., (1998) *not published*

52. Lee, C. T. and Duerre, J. A. (1974) *Nature*. **251**, 240-242.

Figure 1: Morphological transformation of OP27 cell line when treated with R.A differential media and shifted to a non-permissive temperature at 39°C for various lengths of time (Day 0 – Day 10).

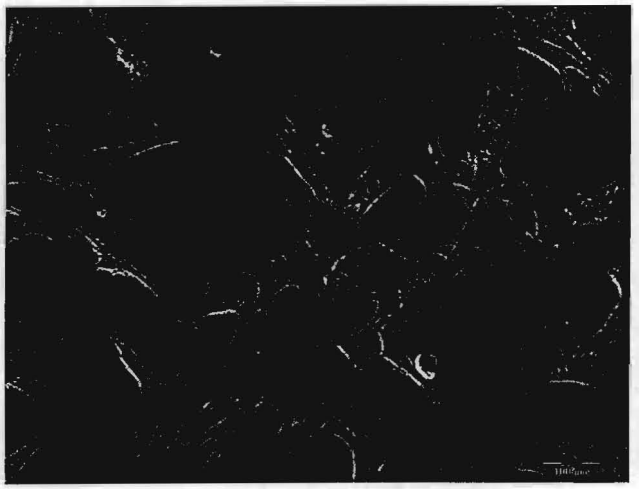

Normal Morphology at 33°C

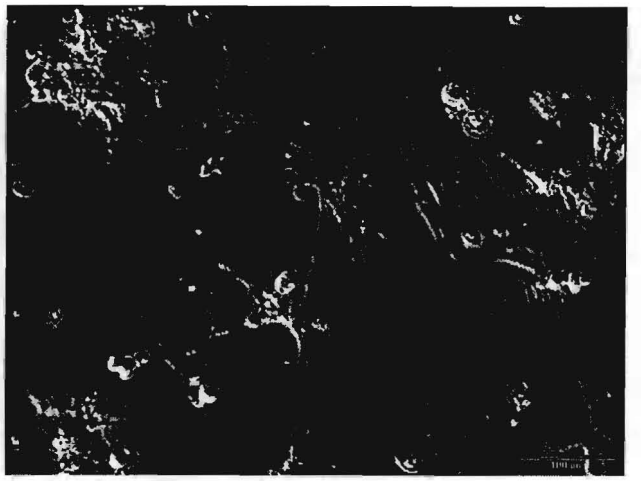

Day 0

Day 1

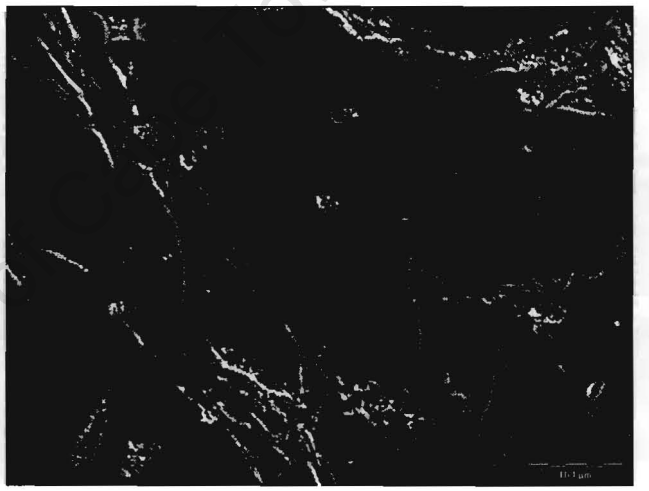

Day 2

Day 3

Day 4

Day 5

Day 6

Day 7

Day 8

Day 9

Day 10

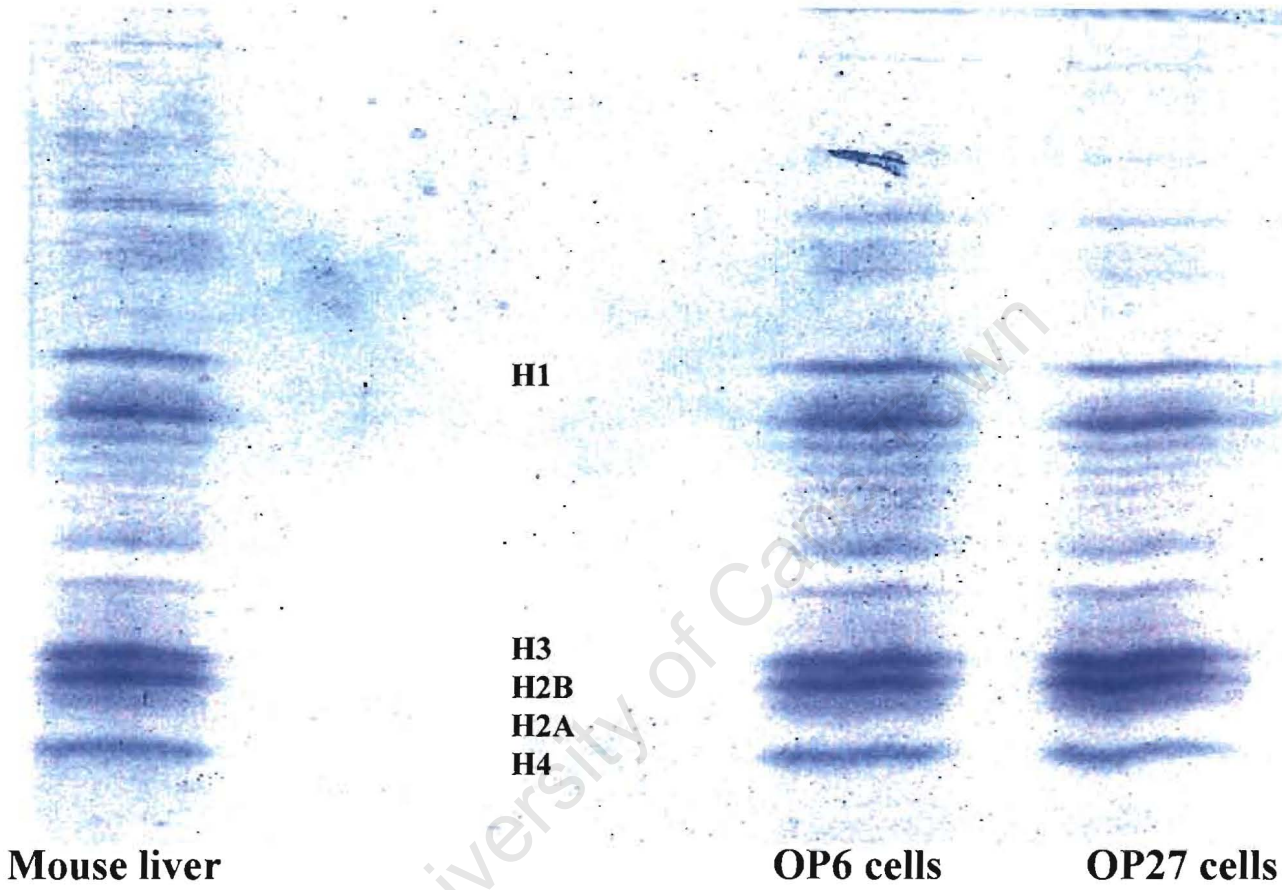

Figure 2.1:

20% SDS-PAGE showing total histones isolated from mouse liver (lane 1), OP6 (lane 2) and OP27 cells (lane 3). Mouse liver histones were extracted with the traditional nuclei extraction method and modified extraction method was used to purify histone OP6 and OP27 from the cell line.

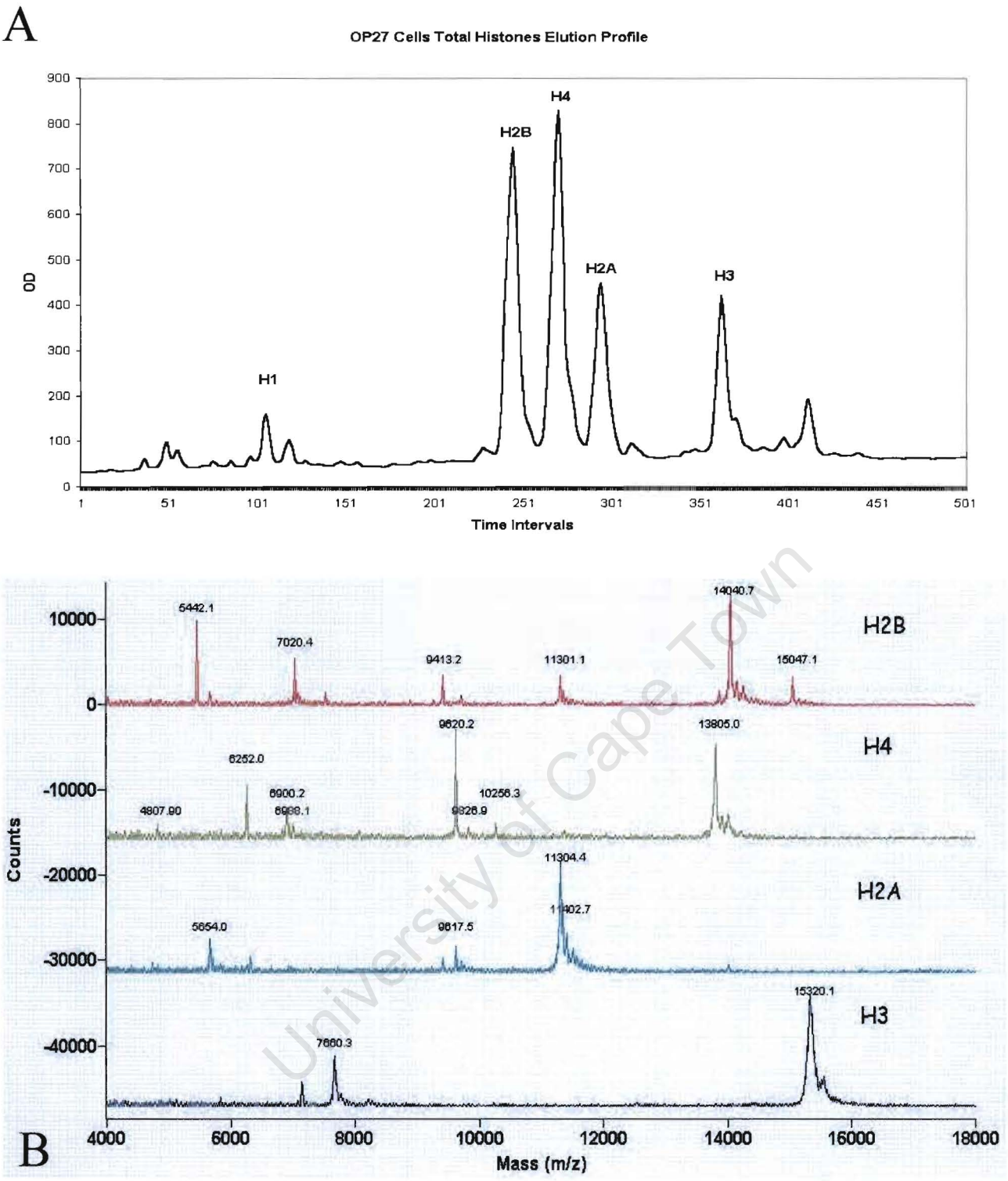

Figure 2.2:

(A) HPLC elution profile of total histones purified from the OP27 cell line. Histone H2B eluted at 55th minute, histone H4 at 56th minute, histone H2A at 58th minute and histone H3 at 61st minute respectively.
(B) Confirmation of HPLC fractions by MALDI-TOF mass spectrometry; peak mass (14040.7 Da) as histone H2B, (13805.0 Da) as histone H4, (11304.4 Da) as histone H2A and (15320.1 Da) as histone H3.

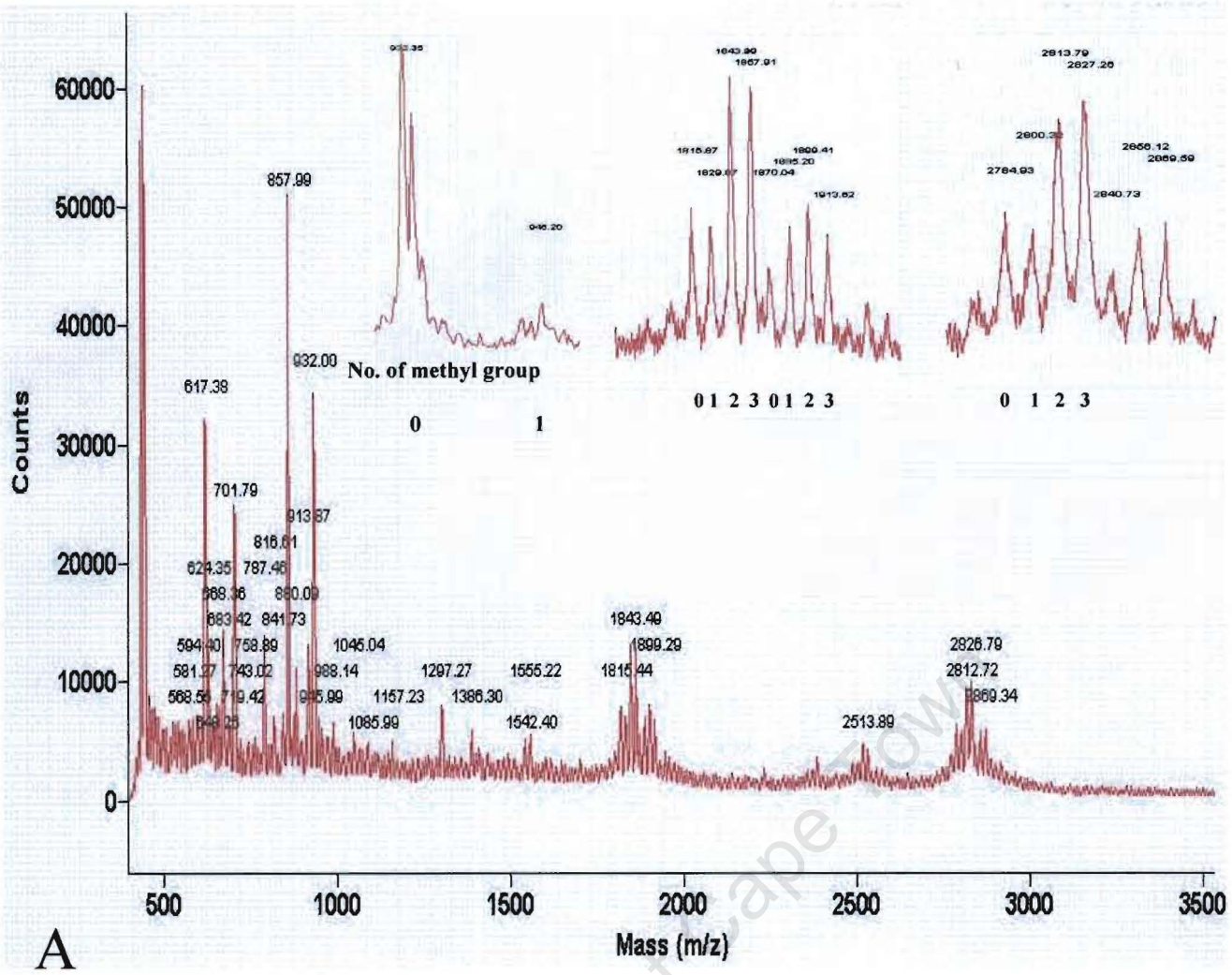

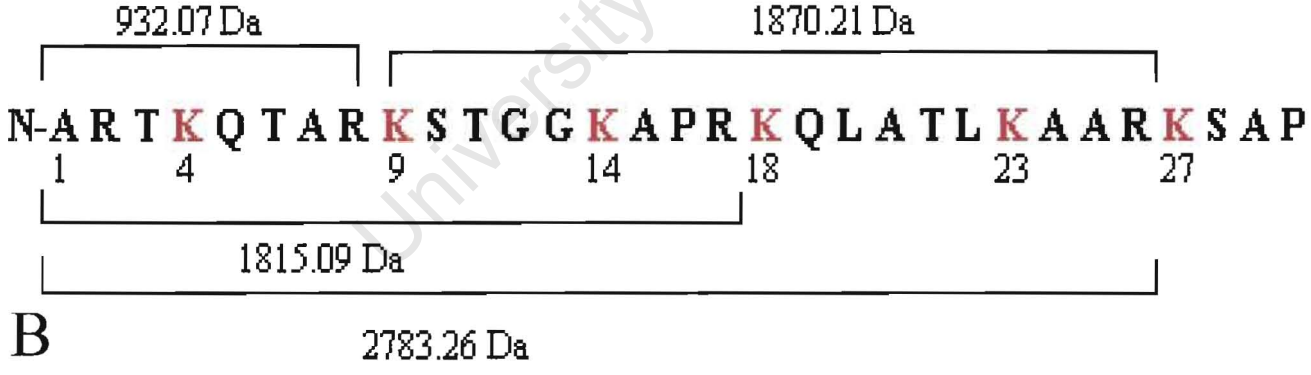

Figure 3:

(A) **A** typical mass spectrometry pattern of OP27 histone H3 digested by Endoproteinase Arg-C. Distinct methylation patterns may be identified after culturing at 33°C. Peak heights of 932.35 m/z (amino acids fragment 1-8) and 946.20 m/z represent the relative abundance of H3 Lys^4 and mono-methylated H3 Lys^4. Peak height of 1870.04 m/z (amino acids fragment 9-26), 1885.20 Da, 1899.41 Da and 1913.62 Da represent the relative abundance of H3 Lys^9, mono-, di- and tri-methylated H3 Lys^9.

(B) **N-terminal** region of histone H3 indicating sites of Endoproteinase Arg-C cleavage and predicted peptide fragments with the respective theoretical masses.

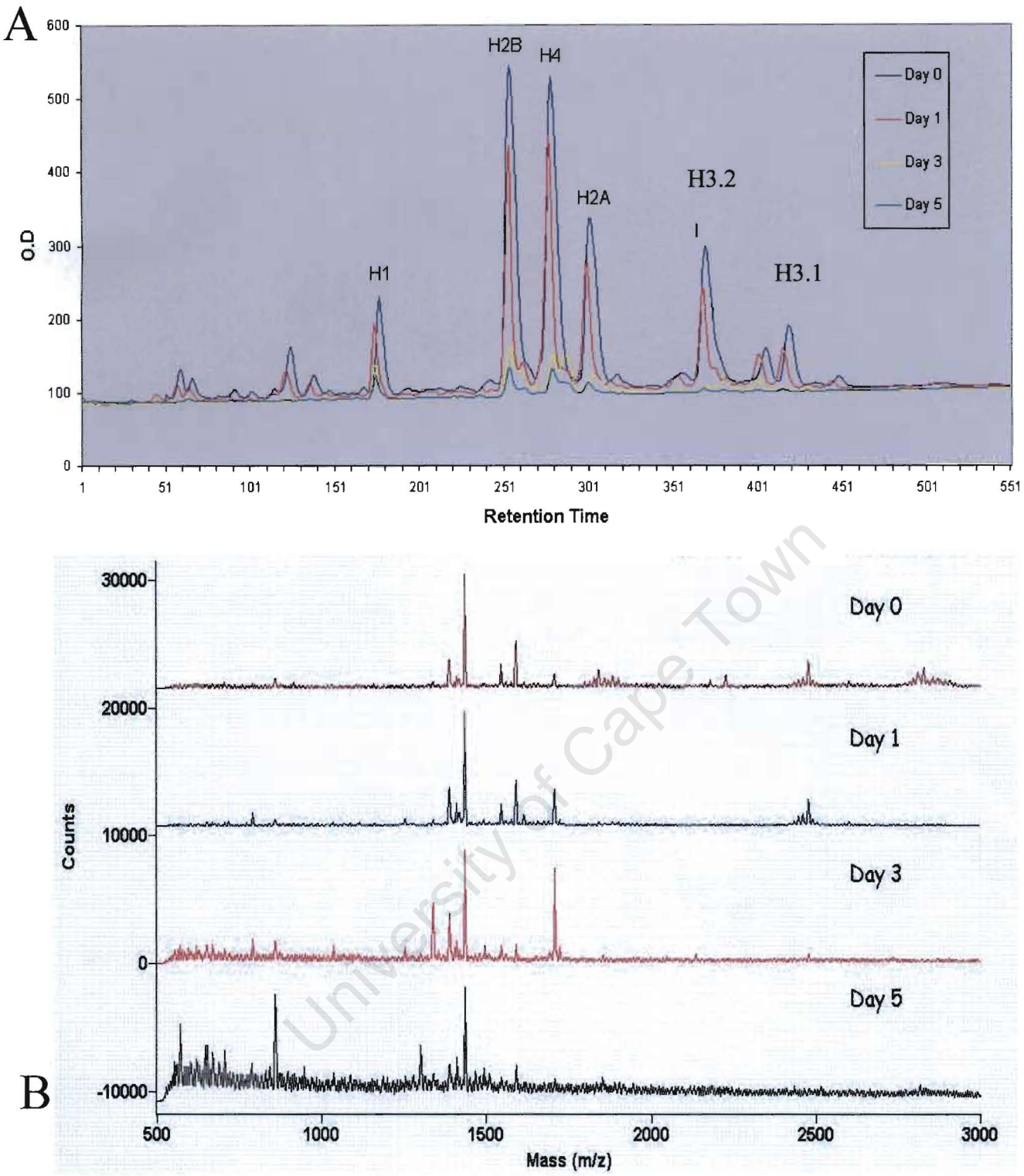

Figure 4.1:

(**A) Comparisons** of reverse HPLC elution profile of OP27 cell line histones (H2A, H4, H2B and H3 respectively) **between** Day 0 (blue), Day 1 (red), Day 3 (yellow) and Day 5 (green). Similar HPLC profiles were obtained for **Day 0** and Day 1, but histones degradation for Day3 and Day 5 can be easily observed.

(B) Comparisons between the MALDI-TOF mass peaks and H3 methylation patterns for Day 0 (brown), Day 1 (blue), Day 3 (red) and Day 5 (black). There are no signs of N-terminal methylation patterns for Day 3 and Day 5.

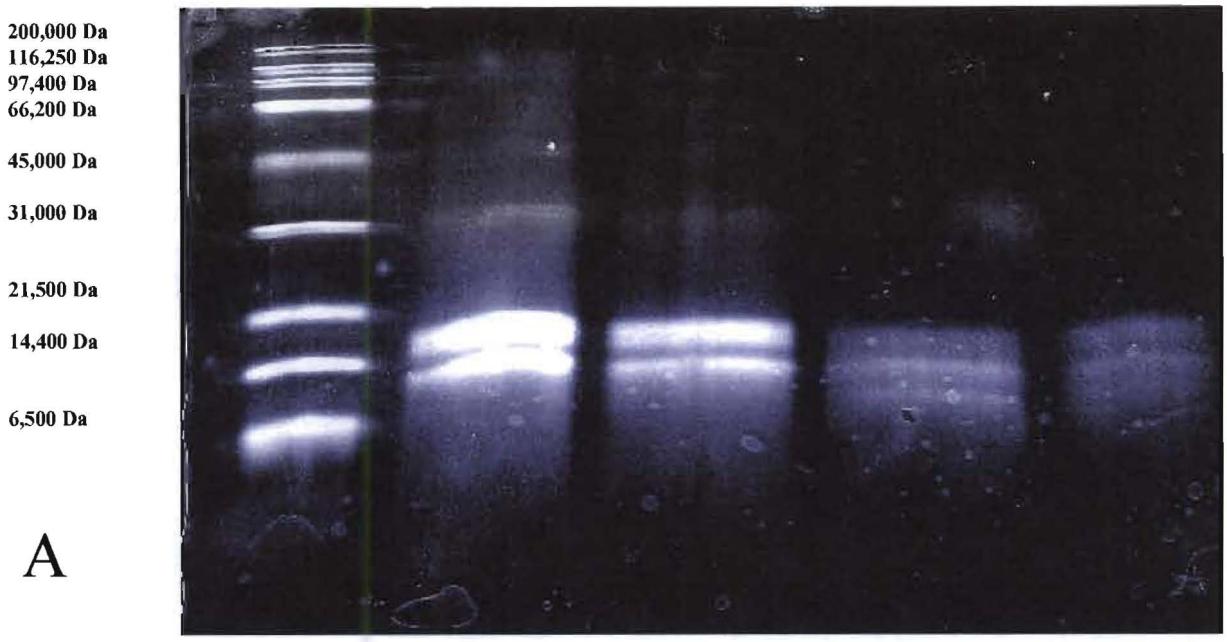

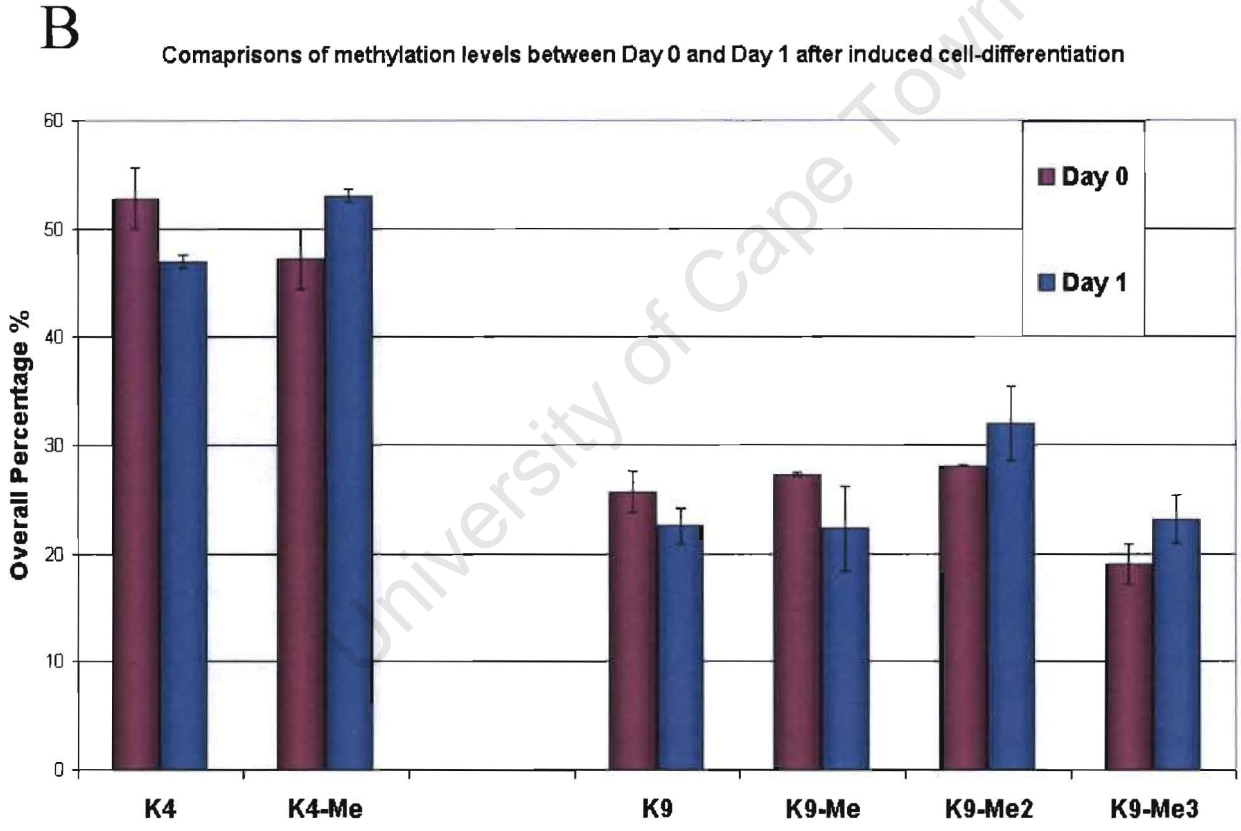

Figure 4.2:

(A) Comparisons of the histone H3 (15,320 Da) for Day 0 (lane 2), Day 1 (lane 3), Day 3 (lane 4) and Day 5 (lane 5) by 20% SDS-PAGE.

(B) Relative percentages of Lys^4, mono-methylated Lys^4, Lys^9, mono-, di- and tri-methylated Lys^9 for Day 0 (purple) and Day 1 (blue). A slight increase in methylation can be observed for both K4 and K9.

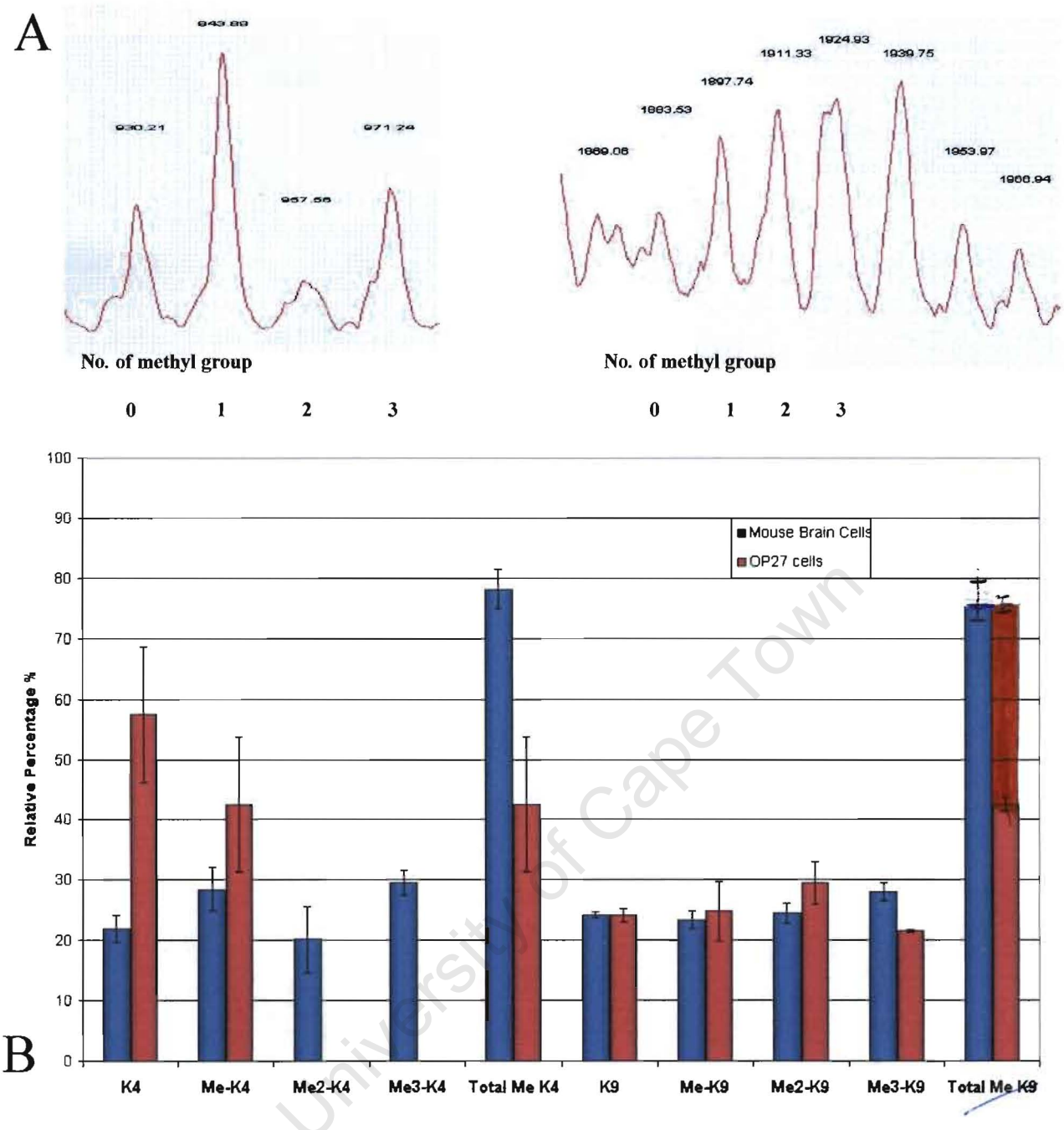

Figure 5:

(A) A typical zoomed in mass spectrometry pattern of mouse brain histone H3 digested by Endoproteinase Arg-C. Peak heights of 930.21 m/z (amino acids fragment 1-8) and 943.90 m/z represent the relative abundance of H3 Lys^4 and mono-methylated H3 Lys^4. Peak height of 1869.06 m/z (amino acids fragment 9-26), 1883.53 Da, 1897.74 Da and 1911.33 Da represent the relative abundance of H3 Lys^9, mono-, di- and tri-methylated H3 Lys^9.

(B) Relative percentage of methylation (mono-, di- and tri-) at Lys^4 and Lys^9 in mouse brain cells (blue) and OP27 cells (red). Data was averaged from 3 sets of mouse brain extracts and 3 sets of OP27 cell extracts. Lys^4 residues in mouse brain are heavily methylated with 20% of di-methylation and 30% of tri-methylation. Lys^9 residues in mouse brain are also slightly more methylated than OP27 cells with approximately 5% more in tri-methylated Lys^9. Overall methylation levels at Lys^4 and Lys^9 for both cells are also compared. Lys^9 residues are equally methylated in both cells, but Lys^4 residues in mouse brain are more heavily methylated than OP27 cells.

Elute	Time (min)	% Buffer B	Flow rate (ml/min)
H1	49	69	0.7
H2B	55	78	0.7
H4	56	80	0.7
H2A	58	82	0.7
H3	61	91	0.7

Table 1:

OP27 total histones elution profile with constant gradient.

Lysine Residue	From-To	Theoretical MH+ (Da)	Averaged Percentage for OP27 (Day 0) (3 sets)	Averaged Percentage for OP27 (Day 1) (3 sets)
Lys^4	1-8	932.07	52.79 ± 2.79 %	46.98 ± 0.59 %
Me-Lys^4	1-8	946.07	47.21 ± 2.79 %	53.02 ± 0.59 %
Total Lys^4 Methylation			47.21 ± 2.79 %	53.02 ± 0.59 %
Lys^9	9-26	1870.21	25.70 ± 1.96 %	22.54 ± 1.68 %
Me-Lys^9	9-26	1884.21	27.23 ± 0.20 %	22.30 ± 3.89 %
Me^2-Lys^9	9-26	1898.21	28.05 ± 0.09 %	31.97 ± 3.40 %
Me^3-Lys^9	9-26	1912.21	19.02 ± 1.86 %	23.19 ± 2.16 %
Total Lys^9 Methylation			74.30 ± 1.02 %	77.46 ± 1.03 %

Table 2:

Relative percentage of methylation at Lys4 and Lys9 in OP27 cells (Day 0 and Day 1). Slight overall increase (6%) in methylation at Lys4 residues and at Lys9 residues (3%) was found after one day in R.A medium. Although there was only a slight increase in overall Lys^9 methylation, but many of the non-methylated and mono-methylated Lys^9 were methylated into the di- and tri-methylated forms (4% increase in both di- and tri-methylated Lys^9).

Lysine Residue	From-To	Theoretical MH+ (Da)	Averaged Percentage for OP27 (3 sets)	Averaged Percentage for Mouse brain (3 sets)
Lys^4	1-8	932.07	57.44 ± 11.17 %	21.88 ± 2.22 %
$Me\text{-}Lys^4$	1-8	946.07	42.56 ± 11.17 %	28.47 ± 3.55 %
$Me^2\text{-}Lys^4$	1-8	960.07	0	20.13 ± 5.40 %
$Me^3\text{-}Lys^4$	1-8	974.07	0	29.52 ± 2.08 %
Total Lys^4 Methylation			48.93 ± 11.17 %	78.12 ± 3.26 %
Lys^9	9-26	1870.21	24.15 ± 1.14 %	24.21 ± 0.46 %
$Me\text{-}Lys^9$	9-26	1884.21	24.80 ± 4.88 %	23.43 ± 1.52 %
$Me^2\text{-}Lys^9$	9-26	1898.21	29.50 ± 3.55 %	24.41 ± 1.67 %
$Me^3\text{-}Lys^9$	9-26	1912.21	21.55 ± 0.19 %	27.96 ± 1.48 %
Total Lys^9 Methylation			75.85 ± 1.14 %	75.79 ± 3.26 %

Table 3:

Relative percentage of methylation (mono-, di- and tri-) at Lys4 and Lys9 in mouse brain cells and OP27 cells. Lys4 residues in mouse brain are heavily methylated with 20% of di-methylation and 30% od tri-methylation. Lys9 residues in mouse brain are also more methylated than OP27 cells with approximately 7% more in tri-methylated Lys9. Overall methylation levels at Lys4 and Lys9 for both cells are also compared. Lys9 residues are equally methylated in both cells, but unlike OP27 cells, Lys4 residues in mouse brain are heavily methylated.

List of Abbreviations

DMEM	Dulbecco's modified Eagle's medium
EDTA	Ethylenediametetra-acetic acid
FCS	Foetal calf serum
GPMAW	General protein/ mass analysis for Windows
HAT	Histone Acetyltransferases
HDM	Histone demethylase
HMTs	Histone Methyltransferases
HPLC	High Performance Liquid Chromatography
Lys^4	Histone H3 lysine residue 4
Lys^9	Histone H3 lysine residue 9
MALDI-TOF	Matrix-assisted Laser Desorption/ Ionization Time-of-flight Mass Spectrometry
MEL	Mouse erythroleukemia cells
MS	Mass spectrometry
OP	Olfactory placode
PBS	Phosphate buffer saline
PDT	Population doubling time
PSD	Post-source decay analysis
RA Media	Retinoic Acid differential media
SAM	S-adenosylmethionine
SDS-PAGE	Sodium dodecyl sulphate polyacrylamide gel electrophoresis
Ser^{10}	Histone H3 Serine residue 10
SV40 Tag	Simian virus 40 oncoprotein large T antigen
TFA	Trifluoroacetic acid
TKM	Tris, potassium, magnesium